Tutor/s

Dr. Juan Carlos Paniagua
Departament de Ciència de Materials i Química Física

Dr. Alberto Credi
Center for Light Activated Nanostructures (CLAN)- Dipartimento di Scienze e Tecnologie Agro-Alimentari

Grau de Química

Treball Final de Grau

Towards the Reversible Electronic Energy Transfer. Synthesis and characterization of nanohybrid Quantum Dots.

Cap a la Transferència d'Energia Electrònica Reversible. Síntesi i caracterització de punts quàntics nanohíbrids.

Gil Murria Aranda

January 2019

Universitat de Barcelona

B:KC Barcelona Knowledge Campus
Campus d'Excel·lència Internacional

“No se puede enseñar nada a un hombre, sólo se le puede ayudar a descubrirse a sí mismo”

Galileo Galilei

A mis padres por todo el apoyo incalculable que me han dado siempre.

Grazie Marcello per avermi dato tanto coraggio per continuare attraverso questo viaggio, anche quando sono arrivate delle “oggettive difficultà”. È stato bello imparare l’italiano.

Grazie Prof. Alberto Credi per avermi dato l’opportunità di essere nel CNR con voi, non mi sarei mai aspettato tanto quando ho fatto la scelta dell’Università.

Gràcies Prof. Juan Carlos Paniagua per atendre'm amb tantes ganes i pels teus suggeriments.

Gràcies Josep per tot el temps que hem passat junts. Tot és un creixement continu.

Gràcies Jon pel teu interès, el valoro molt.

REPORT

CONTENTS

1. SUMMARY

The research presented in this thesis focused on the development of nanohybrids quantum dots for suitable photophysical processes. The supramolecular system consists of an inorganic nanocrystal functionalized with a certain organic chromophore. The photophysical process is based in a bidirectional, that is reversible, energy transfer. For this process to occur, specific energy requirements must be fulfilled, between the emitting state of the nanocrystal and the lowest triplet excited state organic chromophore anchored in its surface. Due to the known value of the energetic state of the organic chromophore, the quantum dot plays a key role. Thanks to the tunability of its photophysical properties regarding the size, it is possible to fulfil this particular synergy. To achieve this objective, CdSe quantum dots functionalized and 2-naphthalene carboxylic acid (2-NCA) were chosen. The nanohybrids were characterized by absorption and luminescence spectroscopy. According to different ratios of ligands, it was possible to modulate the size of different batches of nanoparticles therefore, synthesizing a suitable nanoparticle for the scope of the thesis.

However, the intrinsic instability of the sample regarding the extremely small size led to the impossibility of a comparison between functionalized and non-functionalized the nanoparticle because they no longer presented the same photophysical properties. Despite this, it was possible to verify the presence of the reversible energy transfer through the comparison of the same sample functionalized in deaerated and air-equilibrated conditions. Given that, in deaerated conditions, the nanohybrids showed a higher luminescence intensity in the time-gated detection and a longer luminescence decay in the time scale than the nanohybrids in air-equilibrated conditions.

Keywords: Nanotechnology, quantum dots, supramolecular system, energy transfer, luminescence

2. RESUM

La investigació que es presenta en aquesta tesi ha tingut èmfasi en el desenvolupament de punts quàntics nanohíbrids que presentin certs processos fotofísics. El sistema supramolecular dissenyat consisteix en un nanocristall inorgànic funcionalitzat amb un determinat cromòfor orgànic. El procés fotofísic estudiat, es basa en una transferència d'energia bidireccional, és a dir, reversible. Per a que tingui lloc aquest procés s'han de satisfer uns determinats requisits energètics entre l'estat emissor del nanocristall i el triplet excitat de més baixa energia del cromòfor orgànic que es troba a la superfície d'aquest. Donat que es conegut el valor energètic del cromòfor orgànic, és aquí on el punt quàntic juga un paper clau. Gràcies a la possibilitat de modular les propietats fotofísiques d'aquests materials, a través de la seva dimensió és possible complir amb aquesta sinergia particular. Per portar endavant aquest objectiu, es van escollir com a possibles candidats els punts quàntics de CdSe funcionalitzats amb l'àcid carboxílic 2-naftalè (2-NCA). Els nanohíbrids van ser caracteritzats mitjançant espectroscòpia d'absorció i de luminescència. Segons les proporcions de lligands utilitzades en la síntesi de nanopartícules es va influenciar en la seva dimensió final. Per conseqüent, sintetitzant nanopartícules adients pel propòsit d'aquesta tesi.

Malauradament, la inestabilitat intrínseca de la mostra donada la seva dimensió extremadament petita. No va ser possible comparar les nanopartícules funcionalitzades amb les no funcionalitzades, perquè van deixar de presentar les mateixes propietats fotofísiques entre elles. Tot i això, va ser possible verificar amb èxit que l'energia de transferència reversible havia tingut lloc, per mitjà de la comparació de la mateixa mostra funcionalitzada amb la presència d'oxigen i sense. Ja que en absència d'oxigen els nanohíbrids van presentar una intensitat luminescent més alta en detecció tipus "time-gated" i un decaïment del temps de vida de la luminescència major en escala de temps que essent l'oxigen.

Paraules clau: Nanotecnologia, punts quàntics, sistema supramolecular, transferència d'energia, luminescència.

3. INTRODUCTION

Nanoscience and its related (nano)technology are the investigation and the application of extremely small systems that can be exploited all over different scientific research fields, such as chemistry, biology, physics and materials science.

The basic ideas of nanoscience and nanotechnology were first discussed in the famous Richard Feynman's speech "There's Plenty of Room at the Bottom" during the American Physical Society meeting at the California Institute of Technology (CalTech) in 1959[1]. The revolutionary concept of the speech was the possibility of manipulating and controlling atoms and molecules even at the single-object domain. However, it is worth noting that the word "nanotechnology" was introduced for the first time by Norio Taniguchi of the University of Tokyo in 1974 and that the prototypical molecular-device was developed exactly in the same year. Finally, it is commonly recognized that the so called nanotechnological revolution started with the development of both Scanning Tunneling Microscope (STM) and Atomic Force Microscope (AFM) in 1981[2-3].

Although the terms nanoscience and nanotechnology are quite young, nanosized materials have been used for along time. For example, alternate-sized gold and silver particles were used to create colours in the windows of medieval churches hundreds of years ago, but the artists back then simply did not comprehend that the process they were using to create these artworks actually led to changes in the composition of the materials they were working with.

Modern scientists and engineers are looking for a wide variety of procedures to deliberately produce nanostructured materials to take advantage of their enhanced properties such as higher strength, lighter weight, increased control of light spectrum, and greater chemical reactivity than their larger-scale counterparts.

As already mentioned, nanotechnology is basically a multidisciplinary field connecting different scientific domains and, because of that, the potential applications of nanotechnology promise a really high-impact in areas such as electronics, medical and healthcare, energy, environmental remediation and future transportation benefits. Among all the nanostructured materials which are object of an intense investigation, luminescent semiconductor nanocrystals

quantum dots represent an emerging class of nanosized products that can be of high interest for application in a wide range of fields including nanomedicine, photovoltaics, photocatalysis, lighting and sensing devices. At this point it is worthy to note that Samsung has already launched for the mass marketing a new category of ultrathin television based exactly on the above-mentioned nanocrystals.

3.1. SEMICONDUCTOR NANOCRYSTALS QUANTUM DOTS

Any semiconductor material is a bulk crystalline or amorphous solid, whose band gap typically ranges between that of a metallic bulk material and that of an insulator one (e.g., in the range of 0.5 eV- 3.0 eV). Because of that, one electron can be promoted from the valence band (i.e., the highest occupied band) to the conduction one (the lowest unoccupied band) by providing either thermal energy (e.g., thermoconduction) or a photon of suitable energy (e.g., photoconduction), as a consequence a hole will be left in the valence band thus leading to the formation of a charge-carrier pair defined exciton (see Figure 1). Moreover, the distance between the electron and the hole is defined Bohr radius and represents one of the main physical properties of any bulk semiconductor material.

The recombination of the exciton through the band edge will ultimately lead to the emission of a photon.

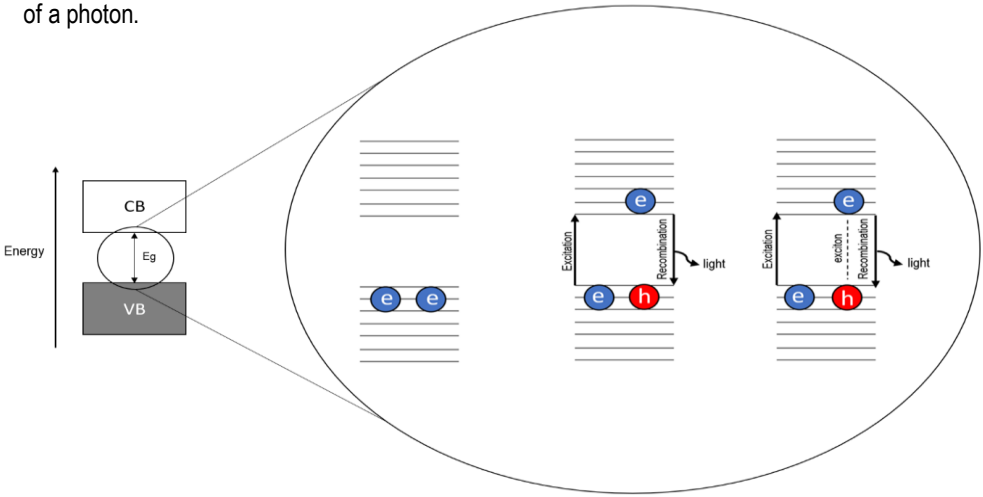

Figure 1. Scheme of the electronic structure of a bulk semiconductor and its two ways of light emission. Being the CB (Conduction Band), VB (Valence Band), Eg (Energy Gap), e (electron) and h (hole). Modified from [4].

However, if the size of a certain bulk material approaches the above-mentioned Bohr radius; the so-called quantum confinement effect starts playing a fundamental role, or in other words starts affecting the properties of the starting material. From an electronic energy point of view, the quantum confinement effect results in the presence of discrete levels within both the valence and the conduction bands, thus leading to a novel configuration between those of the corresponding parental bulk material and general molecules, as shown in Figure 2. Moreover, as the nanocrystal size decreases its bandgap increases ultimately leading to nanomaterials with unique size-dependent optical properties. Such a particular configuration can be described mathematically with the Particle in a box model[5].

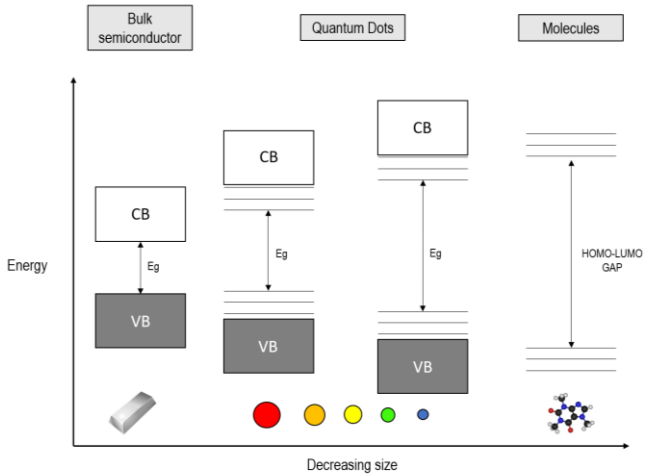

Figure 2. Schematization of the electronic energy configuration of semiconductor bulk materials on the left, quantum dots in the middle and general molecules on the right. Being the CB (Conduction Band), VB (Valence Band), Eg (Energy Gap), HOMO (Highest Occupied Molecular Orbital) and LUMO (Lowest Unoccupied Molecular Orbital).

Finally, it is possible to distinguish, depending on the entity of the confinement itself, between:

- Quantum well, if only one dimension is brought to the nanoscale; then, the resulting structure turns out into an extremely thin films;
- Quantum wire, if two dimensions are brought to the nanoscale; then, the resulting structure turns out into an extremely thin tube/rod/wire;

- Quantum dot, if all the dimensions are brought to the nanoscale (i.e., all the matter is confined in a single point); then, the resulting structure can be referred to as zero dimensional.

Since this thesis focused on the development of luminescent semiconductor nanocrystals endowed with particular photophysical properties, the synthesis, the role of the surface and the functionalization post-synthesis of quantum dots will be described in the next paragraphs.

3.1.1. The general synthetic protocol

Quantum Dots (QDs) are commonly synthesized through the so-called hot injection method reported by Murray and co-workers in 1993[6]. Such a method can be simply referred to as three-steps method:

- **Precursors activation**: namely, the thermal decomposition of the metallic source (e.g., cadmium) in order to obtain the formation of monomers in the presence of suitable organic surfactants;
- **Nucleation**: the agglomeration of several atoms into crystal nucleus. For simplicity, it will be supposed that all the nucleation takes place in spontaneous density fluctuations of the medium and only in homogenous condition. The driving force of this process is obtained by the equation 1:

$$\Delta G_{TOT} = \frac{4}{3}\pi r^3 \Delta G_v + \Delta G_s \qquad \textbf{(Eq.1)}$$

It is worth noting that the ΔGv (volume excess free energy) and the ΔGs (surface free energy) are opposite in terms of signs; namely ΔGv has a negative value due to the formation of crystal nucleus while ΔGs has a positive value since the energetic state of the organic molecules anchored at the surface should be higher than the inner atoms. The balance of this two contributes depends on the value of the so-called critical radius (r*), which can be referred to as size-limit value below which the nuclei re-dissolve into monomers and above which they start growing, respectively. Such a critical radius is given by equation 2:

$$r^* = -\frac{2\gamma}{\rho kT \ln S} \qquad \textbf{(Eq.2)}$$

Going into details, γ is the superficial tension, ρ crystalline phase density, T the temperature, S the precursors grade of supersaturation. Furthermore, it is possible to describe with the Arrhenius model the steady state nucleation rate J (i.e., the number of critical nuclei per time unit in a volume unit of solution):

$$J = J_0 exp(-\Delta G_c / kT) \qquad \textbf{(Eq.3)}$$

As shown in equation 3, the initial steady rate nucleation, Jo, is affected by the interfacial tension, the reaction temperature. From equations 2 and 3, it is possible to conclude that high temperatures will lead to a small value of r* and high nucleation rates, which ultimately result in the most ideal experimental conditions for establishing a homogeneous nucleation of the nanocrystals.

- **Growth stage**: despite several limits, this stage can be explained by the Classical Nucleation Theory (CNT). The relationship between the growth and the nanocrystal radius can be observed in Figure 3:

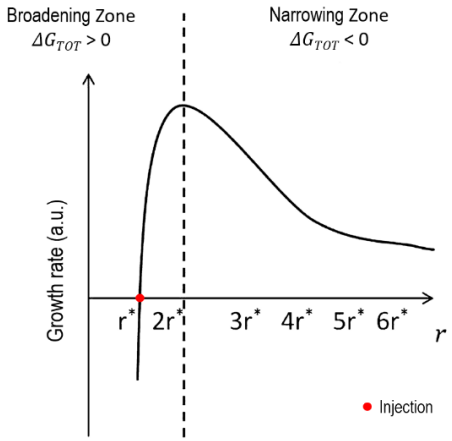

Figure 3. Scheme of the growth rate as a function of the radius value. Showing above of 2r* a distribution narrowing regarding the increasing size. Modified from[7].

It is possible to make several valuable considerations regarding the value of the nuclei radius with respect to the value of r*:

- First case: $r < r^*$: In this stage the agglomeration of small clusters does not equate to the energy barrier for nucleation, thereby the starting crystallites will re-dissolve into monomers.
- Second case: $r^* < r < 2r^*$: In this stage due to the high solubility and the surface energy of smaller particles, they undergo to the Ostwald ripening.
- Third case: $r > 2r^*$: the inverse effect occurs in this stage; namely, the digestive ripening or size focus regime. That is, smaller particles will grow at expense of the larger ones[8].

The most important limit of the application of CNT theory is the treatment of the nuclei as bulk materials thus not considering additional parameters such as the interaction with the surfactants and solvents or the relationship between the γ value and the size. Furthermore, it remains quite difficulty to study the possible mechanism that is taking place due to the high reactivity of these particles (by the high ratio surface/volume).

Due to the intrinsic nature of the nanocrystals, the nucleation and growth rates of these materials are sensitive to a quite large amount of parameters: the nature and concentration of the reactants, the rate of the precursor addition, the temperature of the different synthetic steps, the moisture of the reaction environment, the presence of precursor non-reacted during the reaction, the nature of the coordinating solvent and even possible impurities in reactants with a 99% of purity reported[9]. The different effects that these conditions have made the synthetization of these particles with high reproducibility rather difficult.

3.1.2. The importance of the surface

The choice of the organic surfactants plays a crucial role in preparing semiconductor nanocrystals quantum dots with desired properties. One of the main issues of engineering high quality QDs is the presence of the so-called dangling bonds arising from the unsaturated surface atoms which have less neighbours than their inner counterparts and negatively affecting the photophysical properties of the nanocrystals, such as the emission quantum yield (QY). Since these electrons which do not have any interaction with their counterpart lead to the presence of molecular orbitals (i.e., energetic levels) between the VB and CB, also called trap states. Consequently, the trap states prevent the exciton recombination when is generated due to the absorption of light. One possible solution is to passivate the surface by either overgrowing a shell of another semiconductor or coating the surface with suitable organic ligands[8].

The most commonly used organic ligands or surfactants are intrinsically amphiphilic molecules consisting of both a polar moiety and long aliphatic chains; thus, alkyl amines, alkyl phosphines and fatty acids represent all potential candidates for the choice of the surface ligands[8]. At this point it is important to distinguish between the function of the polar head and the apolar tail of any surfactant molecule: the first one is responsible for the binding interaction with the nanocrystal surface while the second one is responsible for the colloidal stability of the nanocrystals themselves, since it prevents their aggregation.

The outer layer of surfactants can also affect both the chemical-physical properties and the photophysical ones of QDs. It is easy to understand, for instance, that the long aliphatic chains of the surfactants can provide a significant solubility of the nanocrystals only in organic apolar media such as chloroform, toluene and hexane and, depending on their intrinsic steric effect, an efficient surface passivation. As already mentioned, the surface atoms are not fully coordinated and, thus, the more efficient the surface passivation afforded by the organic layer the lower the density of unsaturated atoms and, finally, the better the photophysical properties of the nanocrystals. Finally, it is worth considering that the amount of the organic ligands is responsible of the shape of the resulting nanocrystals[10-11].

3.2. ELECTRONIC ENERGY TRANSFER-BASED QUANTUM DOTS NANOHYBRIDS

A fundamental characteristic of the interaction between the nanocrystals and the organic surfactants, which was not introduced above, is its dynamic nature, which can be exploited to exchange the starting capping agents with new ones in order, for instance:

- to improve the water-solubility of nanocrystals which are intrinsically hydrophobic, then not soluble at all in polar media, which is by the way a crucial requirement for potential applications in the biomedical field[12].
- to introduce new functionalities with respect to the same bare batch of nanocrystals.

Within the second point, the development of a luminescent chemosensor exploiting the photoinduced energy transfer process between a certain type of luminescent colloidal nanocrystals and a suitably chosen organic or inorganic chromophore bound to their surface[13]. In other words, despite the fact that colloidal nanocrystals and common organic/inorganic chromophores are normally considered opponent's like, they can actually collaborate in order to

design new inorganic-organic nanohybrids that can be of high interest for application in lighting and sensing devices

Since the goal of this thesis has been focused on the development of new inorganic-organic nanohybrids exhibiting an unusual bidirectional energy shuttling process, a brief introduction to the theory of the energy transfer process itself may be useful.

The photo-induced electronic energy transfer (EET) is a process involving a general excited specie D* acting as a donor and, thus, transferring its electronic energy to a different one A in its ground state and acting as an acceptor, which ultimately results in the deactivation of D and the photosensitization of A as shown in equation

$$*D + A \rightarrow D + *A \qquad \textbf{(Eq.4)}$$

Such a process can be referred to as either a bimolecular process if D and A are two independent species or an intramolecular one if D and A are part of the same supramolecular architecture. The electronic energy transfer processes can essentially occur through two different mechanisms, one radiative and the other one non-radiative.

The EET process may occur through two main mechanisms which are discussed in the next paragraphs.

3.2.1. The Förster's Energy Transfer

The Förster's Energy transfer process is a mechanism that can be explained in terms of Coulombic interaction between the oscillating electric dipole of the excited donor with the electric dipole of the acceptor in its ground state. However, in order for the energy transfer process to occur a thermodynamic condition must be met. Namely, the energy difference related to the deactivation transition of the donor must be comparable with the energy difference related to the excitation transition of the acceptor. Such a condition can be referred to as a resonance condition, which is by the way the reason why the Förster's Energy transfer is also called Förster Resonant Energy Transfer process.

If such a condition is met, then the excited oscillating dipole of the donor will induce the excitation of the electric dipole of the acceptor in its ground state, which ultimately leads to the deactivation of the donor and the simultaneous sensitization of the acceptor. The mechanism whereby the process occurs and its related kinetic constant are reported in [14].

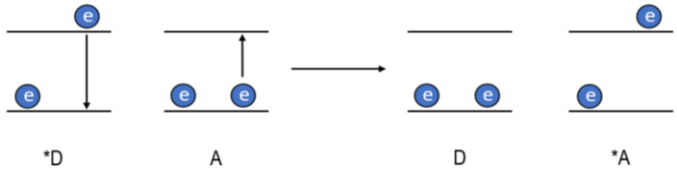

Figure 4. Schematization of the Forster resonant energy transfer process. Modified from [14].

The constant kinetics of the process (k_{en}^{f}) is given by equation 5:

$$k_{en}^{f} = 8.8 \cdot 10^{-25} \frac{K^2 \Phi}{n^4 r_{AB}^6 \tau} J_F \qquad \textbf{(Eq. 5)}$$

The main information provided by the equation is that the speed of the process is inversely correlated to the sixth power of the donor-acceptor distance[14], that is the process itself can be considered as a long-range process (e.g,. it can be efficient until a 5nm range) which doesn't require physical contact between the donor and the acceptor.

Moreover, K is an orientation factor of the dipole-dipole interaction, Φ and τ are, respectively, the emission quantum yield and the life time of the donor in the absence of the acceptor, n is the index of solvent refraction, r_{AB} is the donor-acceptor distance and J_F is the Förster overlap integral between the emission spectrum of the donor and the absorption spectrum of the acceptor.

The photophysical process FRET is spin-allowed, so there is not any change of spin among the acceptor and donor specie during the energy transfer.

Finally, from a quantum-mechanical point of view the Förster's mechanism is allowed if the spin moment of the two partners does not change as shown in equation 6.

$$^*D\ (S_1) + A\ (S_0) \rightarrow D\ (S_0) + {}^*A\ (S_1) \qquad \textbf{(Eq.6)}$$

3.2.2. The Dexter's Energy Transfer

The Dexter's type energy transfer can be described as a simultaneous electron transfer process from the donor to the acceptor and vice versa. Because of that, such a mechanism is also called as exchange process and requires physical contact between the two partners in order

for the electronic orbitals to overlap each other. The mechanism and its related kinetic constant are reported in [14].

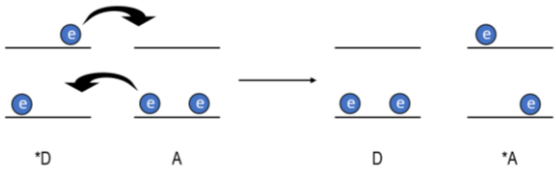

Figure 5. Schematization of the Dexter energy transfer process. Modified from [14].

The constant kinetics of the process (K_{dexter}) is given by equation 7:

$$K_{dexter} = KJ_{exp}\frac{-2R_{DA}}{L} \quad \textbf{(Eq.7)}$$

J is the normalized spectral overlap integral. The term "normalized" here means equalizing the absorption spectra and the emission spectra to the same scale and also obtain the same highest level. K is an experimental factor, R_{DA} is the distance between D and A, and L is the sum of van der Waals radii. Comparing rate constants (equation 5 and equation 7) of different energy transfer models, it is worthwhile to notice that the rate constant of exchange energy transfer decays abruptly because of its intrinsic exponential relationship. Thereby, this is the reason why the exchange energy transfer is also called the short-range energy transfer and the Förster mechanism is called the long-range energy transfer.

The Dexter-type obeys the Wigner's rules, which state that the total spin momentum of the donor-acceptor supramolecule must be unchanged. Such a condition makes, thus, possible a process where even electronic states inaccessible are involved. A typical example of a Dexter's type energy transfer is the one called Triplet-Triplet energy transfer, schematized below.

$$^*D(T_1) + A(S_0) \longrightarrow D(S_0) + {}^*A(T_1) \quad \textbf{(Eq.8)}$$

3.2.3. Reversible Electronic Energy Transfer (REET)

The EET process, as explained previously, relies only on the forward transfer from the donor to the acceptor. However, if certain thermodynamics and kinetic conditions are met, the

forward energy transfer can be followed by the backward one, namely from the acceptor to the donor, thus establishing an equilibration between the two excited states involved or, in other words, to the so called Reversible Electronic Energy Transfer (REET). This particular process is schematized in Figure 6.

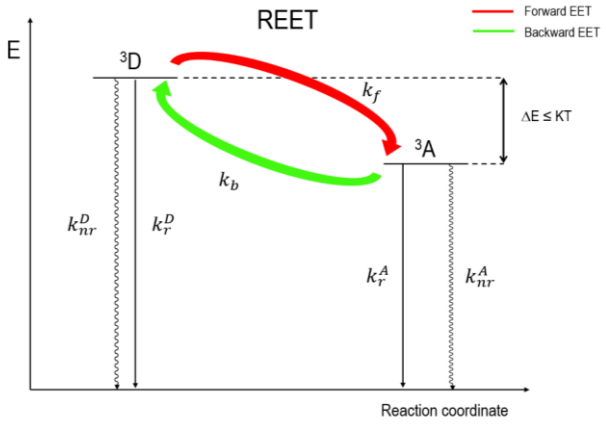

Figure 6. Schematization of the Reversible Electronic Energy Transfer[15].

Considering the thermodynamic requirements, the two excited states involved must be as close as possible in energy; namely their ΔE must be equal or lower than the thermal energy related to the Boltzmann equation (K_BT) in order for the backward energy transfer to be thermally allowed and thus to occur. In other words, such a difference must be lower than few kcal per mol. Obviously, the higher the ΔE the lower the efficiency of the backward energy transfer itself.

Considering the kinetic parameters, it is required to consider that both the donor and the acceptor may deactivate both radiatively and not radiatively; if, for simplicity, only one rate constant is considered for the two components, then the following condition must be satisfied:

$$k_f, k_b > k_D >> k_A \qquad \textbf{(Eq.9)}$$

The previous equation states that, the kinetic constants of the two energy transfer processes k_f and k_b must be comparable and, in any case, higher than the intrinsic deactivation rate constants of the donor and the acceptor themselves.

Once the thermodynamic and kinetic conditions are fulfilled, the forward energy transfer will be followed by the backward one thus leading to a reversible energy shuttling between the donor

and the acceptor. As a consequence, the observed luminescence lifetime will be affected by this energy repartition as stated in the following equation:

$$\frac{1}{\tau_{obs}} = \alpha \frac{1}{\tau_{\mathrm{D}}} + (1- \alpha) \frac{1}{\tau_{\mathrm{A}}} \qquad \textbf{(Eq.10)}$$

The observed lifetime (τ_{obs}) now corresponds to the sum of the donor and acceptor contributes (τ_{D} and τ_{A} respectively) weighed for the repartition value α. One may predict that, if the intrinsic lifetime of the acceptor is much longer than that of the donor, then the main experimental result will be the elongation of the lifetime of the donor by several orders of magnitude, with the acceptor playing the role of energy reservoir of storage component.

4. OBJECTIVES

As already mentioned, QDs have the enormous advantage that their emitting state can be manipulated by changing their size. Because of that, QDs are a potential candidate for engineering new inorganic-organic nanohybrids exhibiting the already described REET process. Then, during the internship at the University of Bologna, my work focused on the development of new CdSe-based inorganic semiconductor nanocrystals decorated with a suitable organic dye, such as 2-napthoic acid.

The project can be then schematized as following:

- Photophysical characterization of 2-napthoic acid (2-NCA).
- Synthesis of CdSe QDs endowed with an emitting level as much as possible close in energy to the lowest triplet excited state of 2-NCA.
- Development of new CdSe@2-NCA nanohybrids to characterize through Uv-vis absorption and luminescence spectroscopic techniques (for a description see chapters 5.3 and 5.4).
- Investigate the possibility for the REET process to occur.

5. MATERIALS AND EXPERIMENTAL METHODS

5.1. CHEMICALS AND REAGENTS

Quantum dots were prepared from the reaction of a metal oxide, organic surfactants and non-metal in its elemental form. Cadmium oxide (CdO, 99%) as metal source, elemental selenium (Se, powder) as non-metal source. Stearic acid (SA, 98%), oleic acid (OA, 90%) as carboxylate sources. Hexadecylamine (HDA, 98%) as base source. 1-octadecene (ODE, 90%) as non-coordinating solvent. Trioctylphosphine (TOP) as coordinating agent of the non-metallic part and 2-naphthoic acid (2-NCA, 98%) as organic chromophore. The solvents used were the toluene (C_7H_8, 99,7%), methanol (CH_3OH), chloroform ($CHCl_3$), heptane (C_7H_{16}; 99,7%) and hexane (C_6H_{14}; 99,7%). All reagents and solvents were purchased from Sigma-Aldrich and used without further purification.

5.2. PREPARATION OF CDSE QUANTUM DOTS

The CdSe QDs batches were prepared by following the procedure reported by Karel and his co-workers[16]. Going into details, such a procedure involves two different fatty acids for the activation of the cadmium source such as stearic acid and oleic acids

Briefly, if stearic acid is chosen for the activation of cadmium precursor, CdO (26 mg, 0.2 mmol, 1 synthetic equivalent) and stearic acid (177 mg, 0.62 mmol, 3 synthetic equivalents) were mixed in a three-bottle neck flask of 50 mL and heated up to 180ºC, in order for the cadmium precursor to be dissolved in the melt stearic acid. After almost 1 hour at 180ºC, the resulting mixture is allowed to cool down at room temperature in order to obtain a new white substrate. Then, HDA (from 3 to 6 synthetic equivalents) and ODE (10 mL) were added and the resulting suspension is first degassed under vacuum at 120°C for at least one hour to remove both the moisture and the oxygen and finally heated up to 245ºC under nitrogen flow. At this point it is important to note that, such a high temperature can be reached because of the presence of a high-boiling point non-coordinating solvent such as ODE. During the heating the solution turns in a yellow pale colour. Once the temperature reaches the value of 245ºC, a selenium precursor solution prepared by dissolving Selenium powder (158 mg, 2 mmol, 10 synthetic equivalents) in 2mL of TOP (by heating up to 100°C under vacuum) is rapidly injected.

Several aliquots are taken over the time to monitor the reaction which is stopped by adding them in $CHCl_3$, once the desired size-sample is obtained. All the QDs batches were then purified

by repeated cycles of precipitation in MeOH in order to remove the unreacted specie and the excess of the surfactants not coordinate the surface of the as prepared nanocrystals.

On the other hand, if oleic acid is chosen, the synthetic procedure presents several differences with respect to the previous one. Briefly, CdO (26 mg, 0.2 mmol, 1 synthetic equivalent), 175.7 mg of oleic acid (0.62 mmol, 3 synthetic equivalents), HDA (from 3 to 6 synthetic equivalents) and ODE (10 mL) were added in the flask at the same time. The resulting suspension is first degassed under vacuum at 120°C for at least one hour to remove both the moisture and the oxygen and finally heated up to different temperature depending on the solvent chosen for quenching the reaction after only five seconds from the injection of the selenium precursor solution made as already described above. Going into details, the injection temperature was set to 170ºC or 210ºC, if hexane or heptane are used as quenching solvent respectively. The QDs batches obtained in this case are purified by either precipitation or extraction with fresh MeOH.

5.3. Uv-Vis ABSORPTION SPECTROSCOPY

The Uv-vis spectroscopy is based on the investigation of the absorption process occurring upon the interaction between light and matter. In order for this phenomenon to occur the energy of the incident radiation, $E = h\nu$, must correspond to the energy difference between quantized levels of a certain system. Going into details, the absorption in the Uv-vis region provides electronic transitions which ultimately result in the formation of a new unstable chemical specie in its electronic excited state.

From an experimental point of view, the spectrophotometer is the instrument exploited to study the light absorption of molecules or atoms in a given range of wavelengths. On the other hand, from a quantitative point of view, the absorption process can be described in terms of Transmittance (T), that is the ratio of the intensity of the transmitted light over that of the incident one. The absorption spectrum is then obtained by plotting the negative decimal logarithm of the transmittance, that is the absorbance (A), as a function of the wavelength of the incident light. Moreover, the absorbance is related to the sample concentration by the Lambert-Beer law as shown in equation 11:

$$A = - \log T = \varepsilon\, b\, c \qquad \textbf{(Eq.11)}$$

Where c is the concentration in mol L^{-1} of the sample, b the optical path the light passes through, and ε is the molar absorption coefficient, which is typical for each molecule and dependent only on the wavelength. A picture of the spectrophotometer used for the experiments reported in this thesis is reported in Figure 7:

Figure 7. The Perkin-Elmer Spectrophotometer

The main components of any spectrophotometer are:

- the electromagnetic radiation source: in a Uv-vis spectrophotometer two lamps are generally used, a deuterium one for the ultraviolet region and a tungsten one for the visible region;
- monochromator: a device able to isolate a suitable portion of the incident radiation;
- cell compartment: a quartz cuvette with an optical path typically of 1 cm;
- detector: a device converting the residual light signal into electrical current. There are different types of detectors that can be sensitive to heat or photons, among these we remember phototubes and photomultipliers.

The absorption spectra reported in this thesis were recorded using a Perkin Elmer Lambda 750 spectrophotometer in a wavelength range between 250 and 800 nm and using quartz cuvettes with an optical path of 1 cm. All the spectra were recorded both in air-equilibrated and deaerated conditions.

The concentration was calculated with equation 11 and the size of the nanoparticles was calculated from the absorption wavelength of the excitonic peak using the empirical equation 12 reported in the literature[18]. Being D, the diameter of the nanoparticles and λ is the wavelength.

$$D = (1.6122 \times 10^{-9})\lambda^4 - (2.6575 \times 10^{-6})\lambda^3 + (1.6242 \times 10^{-3})\lambda^2 - (0.4277)\lambda + (41.57) \quad \textbf{(Eq.12)}$$

5.4. LUMINESCENCE SPECTROSCOPY

Upon the absorption of a suitable photon, a system in a new electronic excited state is generated. Such a state is not stable and must deactivate to the ground one by either non-radiative or radiative patterns.

The photon-absorption process occurs in the femtoseconds (10^{-15}s) time scale. First, the photon is excited from its ground state into higher electronic state. Then, the deactivation of this excitation can undergo different pathways (see figure of Jablonski diagram for a general molecule). If the deactivation occurs by the release of a photon of the same energy hV, it is called a radiative process. But if it goes through other pathways, the process is considered non-radiative, because there is an increase in entropy. Because the exchange of energy in the system is partial, no photon is emitted. Alternatively, the excited state can undergo vibrational relaxation (v.r.) that will not imply radiative transitions between states.

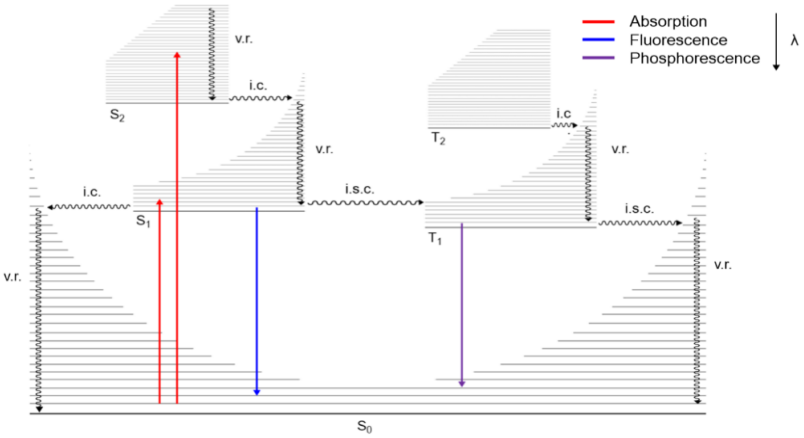

Figure 8. Jablonski diagram for a general organic molecule, modified from [14].

This situation will lead to a competition between the possible different mechanisms in order to deactivate the excited state. But according to the velocity by which one process can occur, some of these processes will be significantly more favoured than others. In the case of the vibrational relaxation, which occurs in an order of magnitude of (10^{-13}s), two main possibilities of deactivation can take place. In the case of v.r. the excited molecule is surrounded by ground-state molecules that tend to dissipate this energy excess through collisions. In the other case, the molecule undergoes an intramolecular vibrational redistribution (i.v.r.). This process implies that

the molecule will act as its own dissipation medium. So, we would have a redistribution of the most populated state by the excitation of the light absorption to other vibrational modes.

As for the non-radiative processes, they can be based on electronic transitions between states that don't have the same spin-multiplicity or between states that have the same multiplicity. Thus, according to these processes, if they obey the spin selection rules, they can be considered as allowed or forbidden processes. It's important to realize that, if the process occurs in one way or another, it will imply a difference in the velocities by which the process is carried out. If the process is spin allowed, then it's called internal conversion (i.c.) in the order of magnitude of picoseconds (10^{-12}s). If the process is not spin allowed, then it is called intersystem crossing (i.s.c.) and the duration can be within the interval of the subnanoseconds or nanoseconds (10^{-9}s). Finally, the deactivations which end in the ground state, experiment a range of duration slower than the i.c. and i.s.c. and are affected by if they obey the spin selection rules (microseconds (10^{-6}s) to nanoseconds) or not (seconds to milliseconds (10^{-3}s)).

The radiative processes, in the same way as the non-radiative processes, can be based in electronic transitions which are spin-allowed or spin-forbidden. If the transition is allowed, then fluorescence occurs, which usually is carried out in nanoseconds. If the transition is not allowed, then phosphorescence occurs, which can elongate to a few seconds.

Given that fluorescence is always originated from the same level, regardless of which electronic energy level is excited. It is worthwhile noticing that, to emit from this level, i.c. process is involved. The same is true for the phosphorescence, but in this case the i.s.c. process is involved. This is the reason why the energy of the emitted photon is usually smaller than the excited photon. Moreover, this fact explains why the fluorescence spectrum is red shifted and can lead to a "mirror image", comparing the absorption spectrum and the fluorescence spectrum. This phenomenon is called Stokes shift and can be influenced by the solvent interactions and temperature[14].

A picture of the spectrofluorometer used for the experiments reported in this thesis is reported in Figure 9:

Figure 9. The Edinburgh FLS 980 spectrofluorometer.

The components of any spectrofluorometer are fundamentally the same of a spectrophotometer. The main differences are the presence of two monochromators for both the excitation and detection procedures, and the relative configuration of the light source with respect to the detector which is placed at 90 degrees instead of 180 degrees as in the case of the spectrophotometer.

The information obtained from the spectrofluorimetric measurements are numerous. First of all, the shape of the emission spectrum with respect to the absorption spectrum and its energy can be rationalized as a function of the distortion of the excited state with respect to the ground one. The more distorted the excited state, the less structured the emission spectrum and the higher the difference in energy between the absorption and the emission spectra; on the other hand, however, if the excited state and the ground state have the same symmetry, the emission spectrum and the absorption spectrum will be almost the mirror image of each other.

The emission spectroscopy acts a complement of the absorption spectroscopy. This it is due to the fact that absorption spectroscopy shows the transitions from the ground state to an excited state, while emission spectroscopy shows the electronic transition from an excited state to the ground state. So, these techniques provide together information about the band gap, exciton binding energies and quantum dot sizes.

Another important parameter that can be obtained from the emission spectrum of any QD sample is the full-width-at-half-maximum (fwhm), which represents the entity of the size-distribution of a given sample. It is commonly recognized that if the fwhm value ranges from 25 to 28 nm any QD sample can be considered well dispersed and the corresponding emission spectrum shows a typical sharp gaussian type profile; on the other hand, if the fwhm is higher than 30 nm then the sample has a worse size-dispersion resulting in a much broader emission spectrum.

The emission spectra reported in this thesis were recorded in a range of wavelengths between 300 and 750 nm with an Edinburgh FLS 980 spectrofluorometer equipped with a Xenon lamp and using quartz cuvettes with an optical path of 1 cm. The delayed emission spectra were recorded using a pulsed μF2 lamp supplied by Edinburgh Instruments.

5.4.1 Determination of the emission quantum yield

The QY (ϕ), is referred to as the ratio of the number of emitted photons emitted (n_E) to the number of photons absorbed (nA).

$$\Phi = \frac{n_e}{n_a} \qquad \textbf{(Eq.13)}$$

As a consequence, the quantum yield ranges from 0 to 1. In the case of QDs the value of the emission quantum yield is affected not only by the size of the sample but also by the density of surface trap state, which represents an alternative pattern of deactivation of the photogenerated exciton.

The quantum emission yields can be calculated using the comparison method with a fluorescence standard[14]. In particular, if the absorbance value of the standard and the sample at the excitation wavelength is the same, the quantum yield can be calculated as in the following equation 14:

$$\Phi_x = \Phi_s \left(\frac{I_s}{I_x}\right)\left(\frac{n_x}{n_s}\right)^2 \qquad \textbf{(Eq.14)}$$

Where Φ is the emission QY, I is the area subtended by the emission band and n is the index of refraction. The subscripts s and x refer to the standard and the sample respectively.

5.4.2 Determination of the luminescence lifetime

As previously mentioned, an excited state is unstable and therefore undergoes a process of decay, in a time scale that ranges from of 10^{-6} to 10^{-15} seconds. The time-correlated-single-photon-counting-spectrometer (TCSPC), or more simply called the single photon, is the instrument used to measure the lifetime of a given sample. The so-called single photon technique

is based on the probability that a single photon emitted by the sample is detected by an appropriate detector. This probability is statistically related to the decrease of the concentration of the excited states over time. The instrument consists of a pulsed excitation source connected to a start photodetector, an excitation monochromator, a sample holder, an emission monochromator, a stop photodetector and a data processing system as shown in Figure 10.

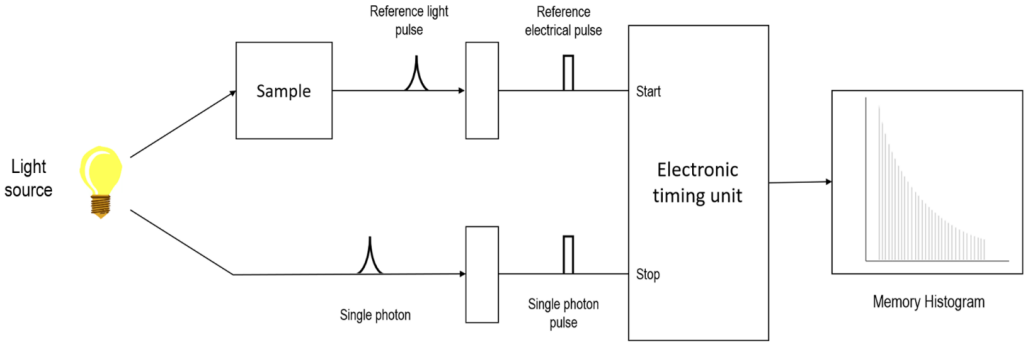

Figure 10. Schematized diagram of single-photon spectrometer.

The technique is as follows: when the source emits a pulse of light, the start photomultiplier sends a signal to the Time Amplitude Converter (TAC) component, which generates a voltage linearly dependent on the time in a range established by the operator. When the first photon emitted by the sample is detected, the stop photomultiplier sends its signal, the voltage variation is stopped and the TAC sends a signal to the analyser that numerically counts the photon, accumulating it in a channel temporally defined by the value of the TAC voltage at the stop time. A new cycle is then starts rising to a high number of counts and to an emission intensity curve as a function of time. This curve coincides with the decay curve of the excited state only if the ratio between the stop signal and the start signal is less than or equal to 0.02; that is, statistically all the photons, regardless of the moment of emission, have a finite possibility of being detected.

6. RESULTS AND DISCUSSION

In this chapter the results obtained during my internship at the University of Bologna are reported and discussed. As already mentioned, the aim of this thesis is the development, namely the synthesis and the characterization of new inorganic-organic nanohybrids consisting of CdSe QDs functionalized with 2-NCA and exhibiting the bi-directional energy transfer process; then, the work focused on the characterization of the ligand and the synthesis of CdSe QDs with a proper size.

6.1. PHOTOPHYSICAL CHARACTERIZATION OF 2-NAPHTHOIC ACID (2-NCA)

Thanks to the photophysical characterization was possible to know the energy value of the lowest triplet excited state of 2-NCA: 2.58 eV which correspond to a value of about 480 in terms of nanometers. As a consequence, in order for the reversible energy transfer to occur, it is required that the emitting state of a proper CdSe QDs sample gets as close as possible to that value.

6.2. PHOTOPHYSICAL CHARACTERIZATION OF THE QUANTUM DOTS SYNTHESIZED

The procedure adopted for synthesizing suitable CdSe QDs was reported by Karel[16] and described in detail in the section 5.2. It is worth noting that I also tried to follow the procedure reported by William Y.[17], Shen H.[18] and their co-workers; however, because of the lack of the reproducibility and the quality of the sample obtained, these methods are not fully useful for the preparation of CdSe QDs with suitable properties. In the next section the results obtained from the synthesis of quantum dots are reported.

6.2.1. First synthesis of CdSe quantum dots batch

Experimental conditions:

- CdO: Stearic acid: HDA = 1: 3: 3
- Injection temperature: 245°C

This synthesis was carried out by exploiting the stearic acid as activating agent of the cadmium source. As already described, whit this protocol it is possible to obtain several different batches of CdSe QDs starting from the same reaction mixture. The absorption and the emission spectra of the as synthesized QDs are shown in Figure 11, their main properties are reported in Table 1 and, finally, the dependence of the first excitonic peak position on the growth time is reported in Figure 12.

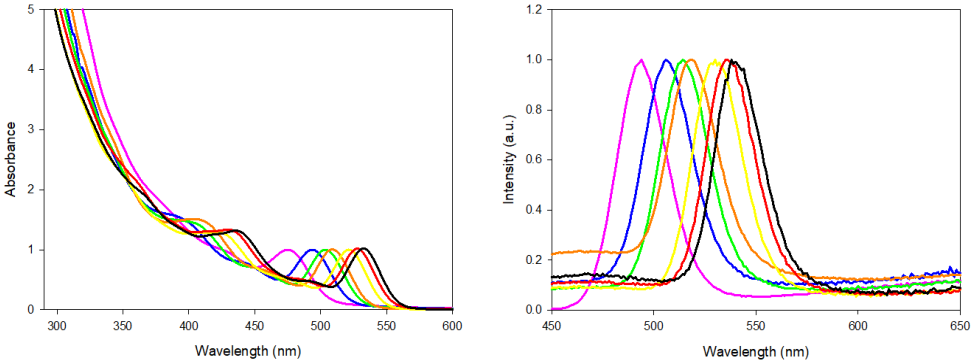

Figure 11. Normalized absorption spectra (on the left) and emission spectra (on the right, λexc = 430nm) of CdSe-1 (purple lines), CdSe-2 (blue lines), CdSe-3 (green lines), CdSe-4 (orange lines), CdSe-5 (yellow lines), CdSe-6 (red lines) and CdSe-7 (black lines). The spectra were all recorded in chloroform.

QDs sample	λ exitonic peak (nm)	Diameter (nm)	Ɛ ($M^{-1}cm^{-1}$)	λ emission peak (nm)	Eg(eV)
CdSe 1	475	2.13	43700	494	2.50
CdSe 2	494	2.29	52600	506	2.45
CdSe 3	503	2.37	58000	514	2.41
CdSe 4	510	2.44	62700	519	2.38
CdSe 5	522	2.58	72700	530	2.33
CdSe 6	530	2.69	81000	536	2.31
CdSe 7	535	2.77	87000	538	2.30

Table 1. Spectroscopic and dimensional data of the CdSe QDs batches.

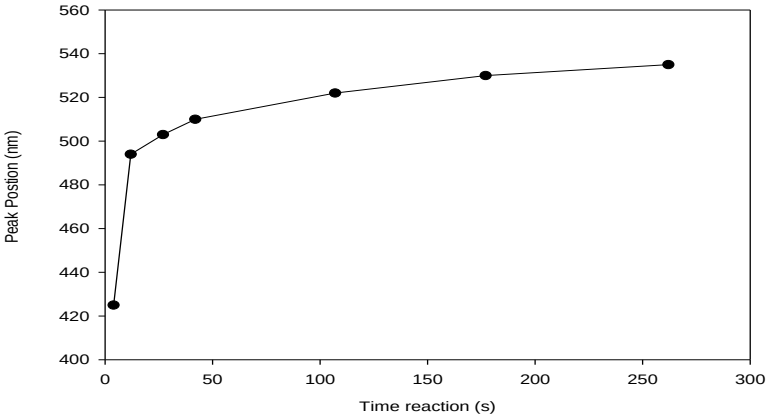

Figure 12. The relationship between the first excitonic peak and the growth time.

The figure 12 underlines how fast is the growth of the nanocrystals within the first 20 seconds after the injection, while the same process slow down after almost one minute.

The second and the third synthesis reported in the next paragraphs are related to the second procedure described in detail in the section 5.2. It is important to remind that the stearic acid is replaced by the oleic acid and the synthesis is quenched by adding a room temperature solvent 5 seconds after the injection. Moreover, the main difference between the second and the third synthesis is the ratio between the surface ligands and the temperature of the hot injection.

6.2.2. Second synthesis of CdSe quantum dots batch

Experimental conditions:

- CdO: OA: HDA = 1: 3: 3
- Injection temperature: 210°C
- Solvent for the quenching: heptane

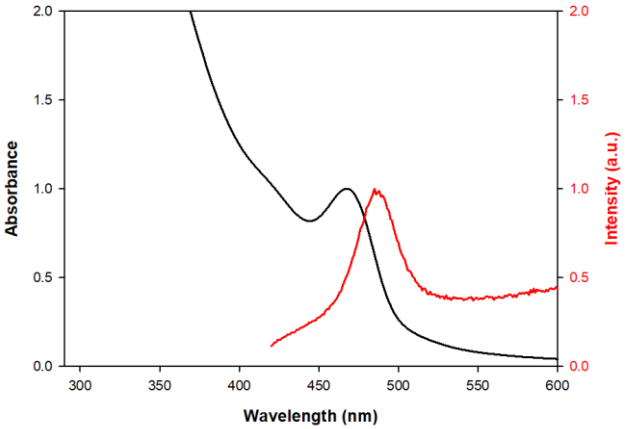

Figure 13. Normalized absorption (black line) and emission spectra (red line, λexc = 400 nm) of the CdSe batch recorded in chloroform.

QDs sample	λ exitonic peak (nm)	Diameter (nm)	Ɛ ($M^{-1}cm^{-1}$)	λ emission peak (nm)	Eg(eV)
CdSe	467	2.07	25400	485	2.55

Table 2 Spectroscopic and dimensional data of CdSe Sample.

6.2.3. Third synthesis of different CdSe quantum dots batches

The last synthesis reported in this thesis can be further schematized as following:

- Depending on the temperature for the hot injection: if T = 170ºC, the corresponding CdSe QDs batch is referred to as “1”. Otherwise, if T =190ºC the corresponding CdSe QDs batch is referred to as “2”.
- Depending on the equivalent ratio CdO: OA: HDA: if such a ratio corresponds to “1:3:6”, the related CdSe QDs batch is referred to as “A”. Otherwise if the ratio corresponds to “1:3:3”, the related CdSe batch is referred to as “B”.

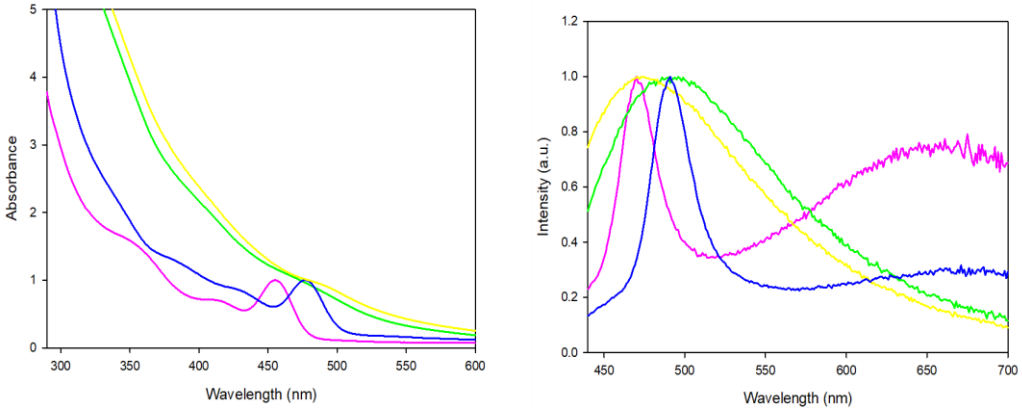

Figure 14. Normalized absorption (on the left) and emission spectra (on the right), of CdSe-1A (purple lines, λ exc = 400nm)), CdSe-1B (green lines λ exc = 420nm), CdSe-2A (blue lines, λ exc = 400nm), CdSe-2B (yellow lines, λ exc = 400nm). All the spectra were recorded in chloroform.

QDs sample	λ exitonic peak (nm)	Diameter (nm)	ε ($M^{-1}cm^{-1}$)	λ emission peak (nm)	Eg(eV)
CdSe 1A	455	1.98	36155	470	2.63
CdSe 1B	473	2.12	42894	496	2.49
CdSe 2A	477	2.15	44549	491	2.52
CdSe 2B	460	2.02	44975	473	2.62

Table 3. Spectroscopic and dimensional data of the quantum dots of CdSe.

As it can be seen in the absorption spectrum, the batch of CdSe 1A shows the synthesis of an extremely small nanoparticles, with low temperature and an increase of base (HDA) regarding the acid (OA) and cadmium oxide. Besides that, the samples which were synthetized with a 1:3:6 ratio show a structured absorption spectrum. In contrast to the batches with a 1:3:3 ratio, which show an unstructured absorption spectrum. Given that it is not possible to observe a well-defined structure in the spectra, the excitonic peak position can be considered as an approximation because there is not any relative maximum trough all the values reported by the spectrophotometer. Thereby, the values reported of the CdSe 1B and CdSe 2B have been

obtained after studying their respective increments of the slope in the absorption spectra and their respective maximums in the emission spectra.

In the case of the emission spectrum, CdSe 1A shows the lowest peak emission, but at the same time the highest contribution due to the contribution of the trap states. It makes sense because the highest contribution is given by the nanoparticle, but a higher number of superficial defects will contribute with an increment of the trap states. At the same time, the ligand ratio influences in the shape of the graphic of the emission spectrum. The quantum dots batches which have the 1:3:3 ratio present high polydispersity in the population of the nanoparticles while the quantum dots samples which have the ligand ratio 1:3:6, present a sharp emission. Thereby, these samples present good monodispersity.

The batches CdSe 1A and CdSe 2B present similar favourable energy gap values by which the two samples would be a potential candidate for the functionalization by acid naphthoic. Theoretically the CdSe 2B showing a polydisperse behaviour in the nanoparticles population would have more chances to be functionalized, because only a small number of nanoparticles population would present a suitable energetic value to carry on the REET. But at the same time, the number of the potential nanoparticles which present these suitable energetic values could be too small. In this sense, if the REET takes place could be that the signal is not intense enough to be detected or to be considered because of the photophysical process. Unlike the CdSe 1A, which shows a bigger number of a potential nanoparticles that could carry on the process. Nor is possible to functionalize one sample after the other one, due to the intrinsic unstable behaviour of the nanoparticles. The population of nanoparticles can reorganize themselves through time varying their own photophysical properties. Moreover, it is almost unpredictable in which direction and how much they will shift from the initial situation.

For all the above explained reasons, the CdSe-1A QDs sample represents a good candidate for preparing new inorganic-organic nanohybrids together with the 2-NCA organic chromophore.

6.3. FUNCTIONALIZATION OF THE CDSE QUANTUM DOTS

The preparation of novel CdSe@2-NCA nanohybrids simply relies on the decoration of the given QDs sample with 2-NCA by taking advantage of their supramolecular assembly occurring at the surface of the nanocrystals. In order for such a post-synthetic functionalization to occur, a mixture of the CdSe nanocrystals and 2-NCA is prepared in toluene, in such a way that the QD/

2-NCA ratio corresponds to 1: 4000. This mixture is then stirred at 45°C, under argon flow, for 65 h. A scheme of this process is shown in figure 15:

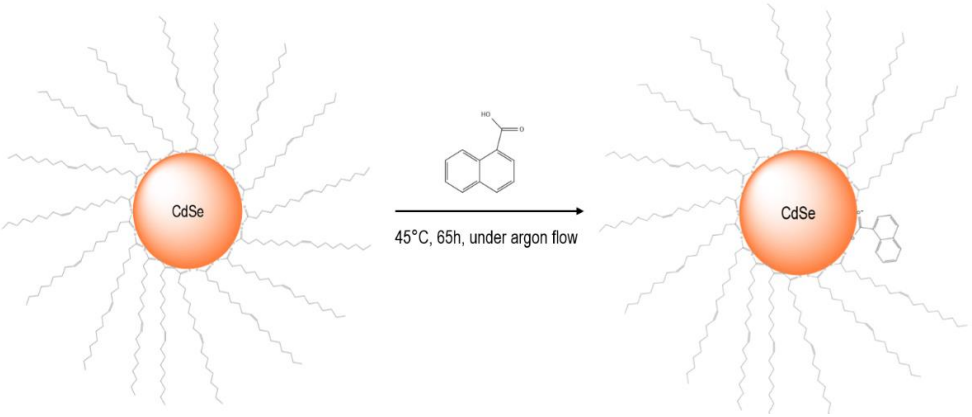

Figure 15. Schematization of the functionalization of the CdSe nanocrystals with 2-NCA molecules.

The next step is the purification, through the Gel Permeation Chromatography (GPC) technique, of the as-prepared CdSe@2-NCA nanohybrids from the excess of the unbound 2-NCA molecules or in other words from the excess of the free ligands. Going into details, a chromatographic column packed with a porous stationary phase such as Bio-Beads SX-1 was prepared.

The GPC method is also a type of size exclusion chromatography (SEC) which provides a separation of the components of any mixture by taking advantage of their different size: namely, the smaller the sample the longer it will be retained by the porous stationary phase. In other words, the SEC mechanism is based on the ability of a given sample to go through the pores of the stationary phase. Obviously, the bigger the sample the less it will be retained by the stationary phase. Therefore, the CdSe@2-NCA nanohybrids elute faster than the excess of the free ligands which will be retained for a longer time. This is the essential advantage of the GPC: being the hydrodynamic size the driving force for the purification rather than the affinity interactions or polarity, it provides a better purification and reproducible results.

The GPC also represents a valid alternative to the most common methods of purification of QDs, such as precipitation by centrifugation or precipitation/redissolution (PR) method, which allows the nanocrystals to be separated from the rest of the molecules which are not directly coordinated with them, simply exploiting the significant difference between them size. For

instance, the repetition of PR cycles could lead to a surface degradation and thus results in the displacement of the native ligands[19].

From an experimental point of view, 4 g of Bio-Beads SX-1 were suspended in toluene overnight for them to swell and then transferred to a column with a section of 1.5 cm and a height of 21 cm and equipped with a proper filter at the bottom. Finally, before starting the GPC, the column is eluted at least three times with fresh toluene to eliminate any contaminants contained in the starting powder. Furthermore, in order to ensure the cleaning of the column an absorption spectrum was recorded. Once the mixture of CdSe QDs and 2-NCA is loaded into the column, the time is monitored through a stop watch. The results obtained are shown in Figure 16:

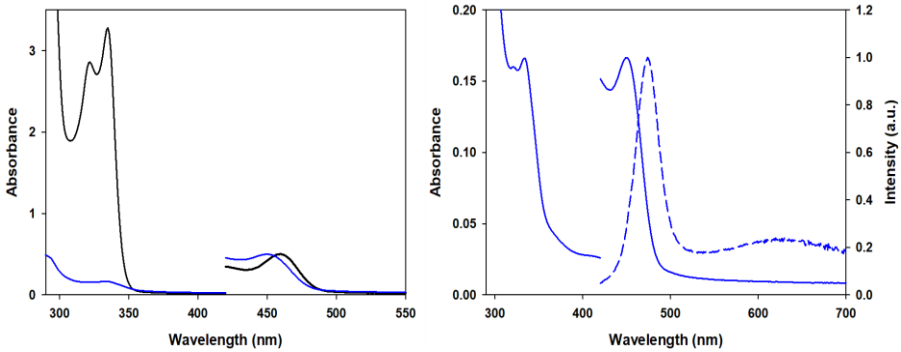

Figure 16. On the left, a normalized absorption spectra of CdSe@2-NCA QDs samples before purification (black line) and CdSe@2-NCA QDs samples after purification (blue line). On the right, a normalized absorption (blue continuous line) and emission spectra (dashed line, λexc = 400 nm) of CdSe@2-NCA QDs samples after purification. All the spectra were recorded in toluene.

The absorption spectra reported in figure 16 show the efficiency of the GPC column. Indeed, if we monitor the signal in the 300-350 nm it is possible to see a significant decrease of the contribution of the 2-NCA ligands, since the excess of the molecule not interacting with the QDs have been removed. At this point it is interesting to note that the time required for the nanohybrids to occur corresponds to 14 minutes which is fully coherent with that of the same unfunctionalized bare batch (i.e., about 16 minutes) while the free ligands leave the column only after 40 minutes.

6.4. REVERSIBLE ENERGY TRANSFER EXPERIMENTS

Once the sample consisting of CdSe@2-NCA nanohybrids was obtained and purified, the work focused on the preparation of two solutions: one of the bare unfunctionalized batch of QDs and the other one of the nanohybrids. Moreover, it was decided to prepare the two samples with the same concentrations, that is with the same absorbance value at the excitonic peak. The strategy simply relies on the comparison between the two samples in order to investigate any possible effect or influence related to the presence of a specific molecule such as 2-NCA on the surface of the nanocrystals with respect to the starting batch.

The absorption and the emission spectra of the as-prepared solution as well as those of the bare batch as synthesized are reported in figure 17.

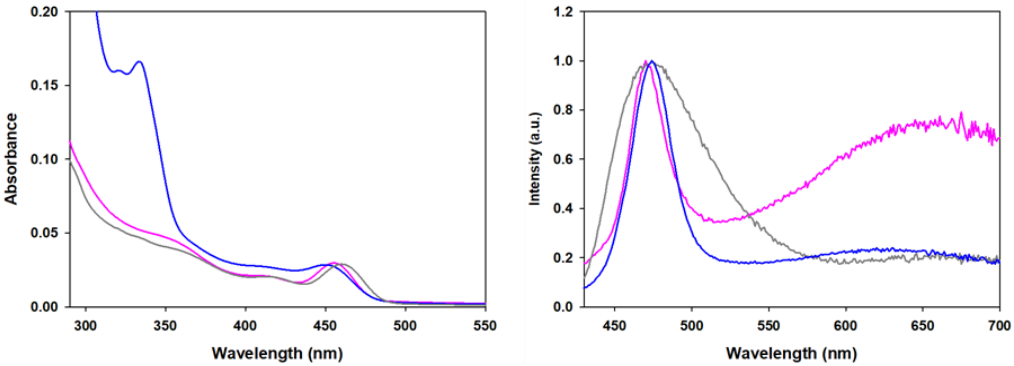

Figure 17. On the left, a normalized absorption spectra of CdSe@2-NCA QDs samples (blue line), CdSe QDs sample after 60 hour (pink line) and CdSe QDs as-synthetized batch (grey line). On the right, normalized emission spectra (λexc = 400nm) of CdSe@2-NCA QDs samples (blue line), CdSe QDs sample after 60 hour (pink line) and CdSe QDs as-synthetized batch (grey line). All the spectra were recorded in toluene.

QDs sample	λ exitonic peak (nm)	λ emission peak (nm)	Eg(eV)
CdSe@2NCA	449	473	2.62
CdSe as-synthetized	455	470	2.63
CdSe after 60 h	460	474	2.61

Table 4. Spectroscopic data of the quantum dots of CdSe.

As already mentioned before, the strategy was focused on the comparison between the CdSe@2-NCA nanohybrids and the starting batch. However, by carefully checking the spectra reported in figure 17 it is possible to make several considerations.

First of all, it is easy to distinguish the contribute of the 2-NCA anchored molecules; indeed, the absorption spectrum of the nanohybrids (see figure 17, blue line) shows an additional absorption band in the 300-350 nm with respect to the starting batch (see Figure 17 pink and grey lines). Moreover, it is possible to observe a slight shift of the excitonic peak both in the absorption and the emission spectra. Such a shift can be first ascribed to the surface decoration with a different ligand compared to the native capping agents.

Nevertheless, the other main consideration is that the bare CdSe QDs batch shows a significant variation after 60 hours, that time corresponds to the preparation of the optically matched solutions. Indeed, it is possible to observe not only a shift in the position of the excitonic peak but also a significant widening of the emission band which is now much broader than the starting one.

This unexpected behaviour can be explained in terms of instability. It is known that the surface to volume ratio increases with the size and, as a consequence, the bigger the nanocrystals the higher their stability. In other words, it is reasonable to say that the starting batch is not so stable and tends to aggregate.

From the results shown in this section it is finally possible to say that the sample corresponding to the starting unfunctionalized batch of CdSe QDs cannot be exploited as a reference batch regarding the funcionalized batch of CdSe QDs, since it now represents a novel different sample of nanocrystals.

At this point, it is important to note that the experiments which are reported below were performed in deaerated solution and by exciting selectively the nanocrystals. These two conditions are now explained in detail.

More specifically, the sample was degassed through the freeze-pump procedure. This technique is based on the inverse dependence of the solubility of any gas specie on the external pressure (i.e., Henry's law). Since lowering the pressure of the gas above the liquids leads to a decrease in solubility of the dissolved gas in the liquid. Then, in order to produce a re-equilibration between the liquid-gas phase, the dissolved gas is released from the liquid as bubble. Briefly, the sample is loaded in a special cuvette endowed with a glass ball which is frozen in a liquid nitrogen bath. This cuvette is then degassed up to 10^{-6} mbar through a powerful vacuum pump connected to a suitable Schlenk line. Once all the equipment is equilibrated and the solution allowed to warm up to room temperature under reduced pressure, so that the oxygen is forced to leave the solution. This procedure is then repeated at least three times. The aim of the freeze-pump thaw is to minimize any possible effect of the presence of the oxygen on the sample investigated.

Regarding the second condition, since the absorption of the nanocrystals overlaps partially with that of the 2-NCA, it is required to excite the sample only where the QDs absorb in order to investigate any possible energy transfer process from the QDs to the ligand, which corresponds to the photoinduced sensitization of the ligand itself, as already explained in section 3.2.

The results shown in figure 18 and 19 arise from the so-called time-gated experiments. If we consider the case of any emission spectrum recorded with a Xenon lamp, we normally talk about steady state experiment, that is, the detector collects any signal related to the sample as long as the light source provides the excitation. In other words, this is an example of stationary measurement or experiment. However, if we move to the time-gated mode, we have to set first two main additional parameters:

- the delay time, which corresponds to a time interval after which the detector starts collecting, if there is, any signal arising from the sample;
- the gate time, which corresponds to a time window during which the measurement is performed.

It is important to note that the delay time is set to avoid any residual signal of the light source, which allows us to investigate both the phosphorescence and the thermally activated delayed fluorescence processes. Any time-gated experiments are also called time-resolved experiment.

Since the main experimental consequence of the reversible energy transfer are the thermally activated delayed luminescence and the elongation of the luminescence lifetime respectively, it is now possible to understand how the work of this thesis has been carried out.

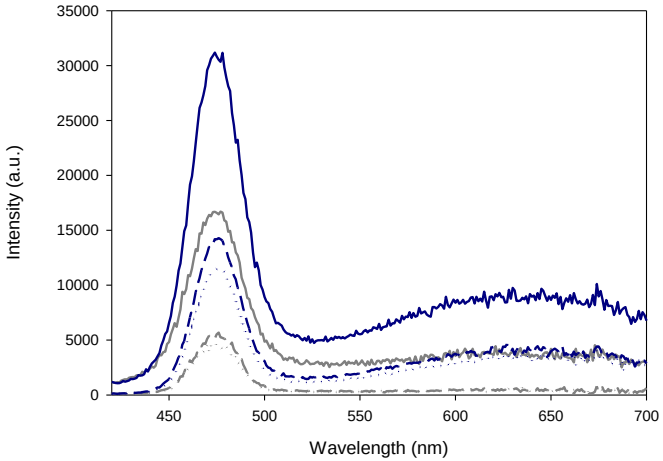

Figure 18. Time-gated emission spectra (λexc = 400nm) of CdSe@2-NCA QDs sample in deaerated (blue lines) and air-equilibrated (grey lines) at room temperature solution, recorded after a delay of 0.04 ms (solid lines), 0.08 ms (dashed lines) and 0.12 ms (dotted lines). The gate time was set to 9 ms.

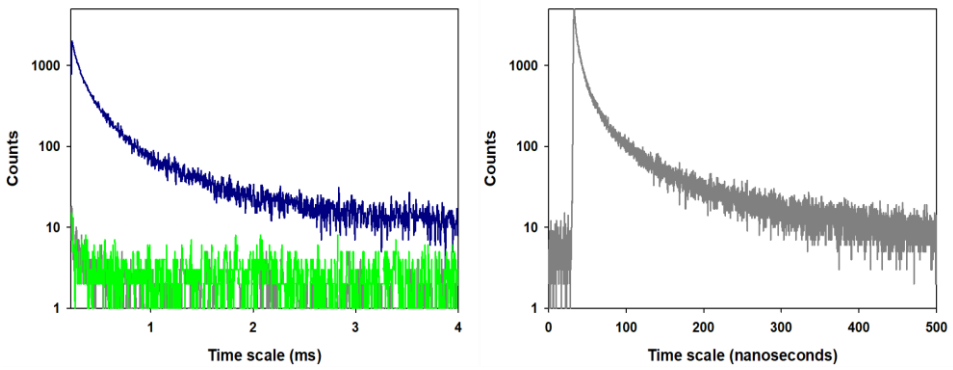

Figure 19. On the left, luminescence decays in the milliseconds domain of CdSe@2-NCA in deaerated (blue line) and air-equilibrated (grey line) solution. The green line is a solution used to scatter the light. Thus, is possible to observe if CdSe@2-NCA in air-equilibrated solution, presents a significant value on the measurements or if it is noise. The excitation is set to 400 nm, the emission monitored at 474 nm, the delay time and the gate window are set to 0.12 ms and 9 ms, respectively. On the right, the luminescence decay in the nanoseconds domain of CdSe@2-NCA in air-equilibrated solution (grey line). All the decays were collected in toluene at room temperature and the counts are reported in logarithmic scale.

As already mentioned, the experiments were performed first in deaerated conditions and then in air-equilibrated one to investigate any kind of influence related to the oxygen. Indeed, it is known that any quantum dots sample is inherently unaffected by oxygen; in other words, the luminescence of the nanocrystals cannot be quenched in any case by oxygen.

However, if we compare the time-gated emission spectra recorded in both deaerated and air-equilibrated conditions, it is possible to observe a clear effect of the oxygen in the luminescence intensity of the nanocrystals. Going into details, the luminescence intensity is still clearly detected even after a delay of 0.12 ms in the absence of oxygen, while the same signal is significantly weak if oxygen is dissolved in the sample; which ultimately results in the fact that because of the presence of the 2-NCA ligands anchored to their surface, the CdSe QDs behave now differently with respect to oxygen. This result may be used, for instance, to develop novel QD-based nanostructure which are sensitive to the oxygen. Furthermore, in order to investigate such an effect, the luminescence decay of the CdSe@2-NCA was collected once again in both deaerated and air-equilibrated solution (see figure 19). The results obtained show a clear decay of the nanohybrids in the milliseconds domain of course provided there is no oxygen in solution (see line blue), otherwise, no signal but only noise can be collected in the same time scale if there is oxygen in solution. Then, if we consider that the luminescence decay of the same sample in air-equilibrated solution can be collected only in the nanoseconds domain it is to understand that the elongation of the lifetime of the nanocrystal is achieved. Moreover, by considering the results from the fitting it is possible to estimate such an elongation to as 5 orders of magnitude at least. In order rationalize these results it is required to see the energetic level diagram reported in figure 20.

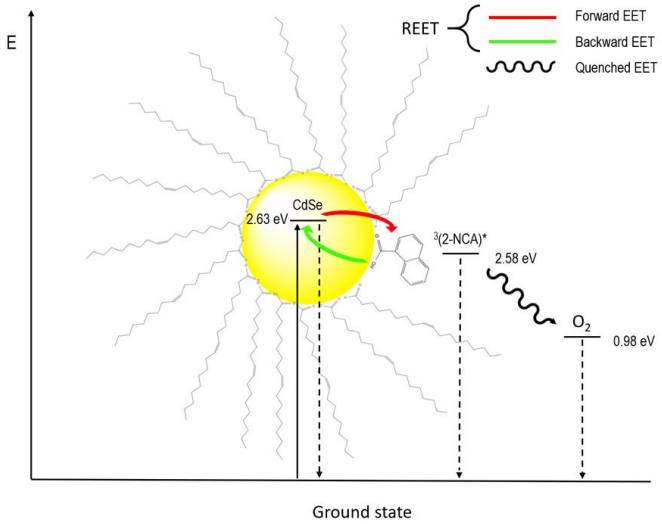

Figure 20. Schematic view of the energy levels of the CdSe, 2-NCA, and oxygen with their respective values in electronvolts. The energetic value of the oxygen was taken from [30].

Since the energy difference between the emitting state of the nanocrystals and the lowest triplet excited state of 2-NCA is less than 0.1 eV, they can be considered almost iso-energetic or energy-matched so that the forward energy transfer occurring upon the selective excitation of the nanocrystals and from the nanocrystals themselves to the ligand is then followed by the thermally allowed back energy transfer process from the ligand to the nanocrystals. This results in the equilibration between the excited states which ultimately results in both thermally activated delayed luminescence and the elongation of the lifetime of several orders of magnitude, provided there is no oxygen in solution. Indeed, it is known that the triplet excited state of any organic chromophore can be quenched by oxygen. Then, if oxygen is dissolved in the solution the triplet excited state of 2-NCA which is first sensitized by the QDs, cannot give back the electronic energy thus preventing the backward energy transfer process and because of that the luminescence intensity of the QDs is quenched (see figure 18) and is no longer possible to detect any luminescence decay in the milliseconds domain (see figure 19).

7.CONCLUSIONS

The synthesis of the CdSe quantum dots was successfully carried out and functionalized with 2-Naphthoic acid. Through the characterization of nanocrystals obtained several conclusions can be considered:

- The method reported by Karel and his co-workers[16] is proven as a valid synthetic method for achieving nanoparticles with suitable photophysical properties to carry the bidirectional energy transfer between the CdSe quantum dots and the 2-Naphtoic acid.
- Low boiling-point solvents used in the hot-injection method lead to smaller nanoparticles.
- Duplicating the amount of hexadecylamine from a ratio of 1:3:3 (CdO:OA:HDA) to 1:3:6 led to structured absorption spectrums and a monodispersing of the nanoparticles population.
- Depending on the ratio of oleic acid and hexadecylamine it is possible to alter the size of the nanoparticles. However, further investigation is needed to understand the effect of the ligands ratio regarding the temperature, since the behaviour showed by the nanoparticles between the ratio and temperature were not correlated.
- It is possible to synthetize CdSe quantum dots with a size smaller than 2nm with the method reported by Karel and his co-workers[16]. The importance lies in the confirmation itself to reproduce these results, given the significative difficulty that implies synthetizing the CdSe nanoparticles with these extremely small dimensions reported by the literature. Moreover, presenting a considerable stability to carry one the photosynthetic procedure.
- The nanoparticles showed an unstable and degradative behaviour in its photophysical properties over time. Thereby it is essential to further optimize the synthetic method in order to consider the yield of the reaction.

8. REFERENCES AND NOTES

(1) Science, E. **1995**. There ' s Plenty of Room at the Bottom.

(2) Binnig, G., & Technical, D. **1987**. Scanning microscopy to, **1986**.

(3) R. Howard and L. Benatar, A Practical Guide to Scanning Probe Microscopy, Park Scientific Instruments, Sunnyvale, CA, USA.

(4) J.W.G. Antonie and J. Olaf (**2017**, January 9). BASIC PHOTO PHYSICS [Blog post]. Retrieved from http://photobiology.info/Visser-Rolinski.html

(5) Spin, E., Goudsmit, S., & Klein, O. **2011**. Introducing Relativity into Quantum Chemistry, *88*(1), 2010–2012.

(6) Murray, C. B., Norris, D. J., & Bawendi, M. G. **1993**. Synthesis and Characterization of Nearly Monodisperse CdE (E = S, Se, Te) Semiconductor Nanocrystallites. Journal of the American Chemical Society, *115*(19), 8706–8715.

(7) Thanh, N. T. K., Maclean, N., & Mahiddine, S. **2014**. Mechanisms of nucleation and growth of nanoparticles in solution. Chemical Reviews, *114*(15), 7610–7630.

(8) Donegá, C. D. M. **2011**. Synthesis and properties of colloidal heteronanocrystals. Chemical Society Reviews, *40* (3), 1512–1546.

(9) Wang, F., Tang, R., Kao, J. L. F., Dingman, S. D., & Buhro, W. E. **2009**. Spectroscopic identification of tri-n-octylphosphine oxide (TOPO) impurities and elucidation of their roles in cadmium selenide quantum-wire growth. Journal of the American Chemical Society, *131*(13), 4983–4994.

(10) Bullen, C., Mulvaney, P., Uni, V., Park, V., Caesar, S., & Allee, L. **2006**. The Effects of Chemisorption on the Luminescence of CdSe Quantum Dots, (11), 3007–3013.

(11) Zhi-bing, W., Jia-yu, Z., Yi-ping, C., Passivation, I., Mohamed, E. H., & Ling, X. **2017**. Ligands Exchange , Studying the Stability and Optical Properties of CdSe / CdS / ZnS Quantum Dots with Liquid Crystal Ligands Exchange , Studying the Stability and Optical Properties of CdSe / CdS / ZnS Quantum Dots with Liquid.

(12) Klostranec, B. J. M., & Chan, W. C. W. **2006**. Quantum Dots in Biological and Biomedical Research : Recent Progress and Present Challenges, 1953–1964.

(13) Silvi, S., Baroncini, M., La, M., & Credi, A. **2016**. Applications. Topics in Current Chemistry, 374(5), 1–27.

(14) V. Balzani, P. Ceroni, and A. Juris, Photochemistry and Photophysics. **2014**.

(15) Denisov, S. A., Yu, S., Pozzo, J. L., Jonusauskas, G., & McClenaghan, N. D. **2016**. Harnessing Reversible Electronic Energy Transfer: From Molecular Dyads to Molecular Machines. ChemPhysChem, 1794–1804.

(16) Dorfs, D., C̆apek, R. K., Poelman, D., Lambert, K., Smet, P. F., Hens, Z., & Eychmüller, A. **2009**. Synthesis of Extremely Small CdSe and Bright Blue Luminescent CdSe/ZnS Nanoparticles by a Prefocused Hot-Injection Approach. *Chemistry of Materials*, *21*(8), 1743–1749.

(17) Zavattini, C., & Zavattini, C. **2003**. Roma , Aç ı k ehir Rome , Open C ı ty Strombol ı Almanya , S ı f ı r Y ı l ı Germany , Year Zero He m ehri Pa ı sa Ekmek , A k ve Hayal Bread , Love and Dreams Aylaklar I V ıt ellon ı Orgosolo Haydutlar ı Band › t › a Orgosolo 2-30 May ı s / May 201, *125*(17), 2854–2860.

(18) Shen, H., Wang, H., Tang, Z., Niu, J. Z., Lou, S., Du, Z., & Li, L. S. **2009**. High quality synthesis of monodisperse zinc-blende CdSe and CdSe / ZnS nanocrystals with a phosphine-free method, 1733–1738.

(19) Shakeri, B., & Meulenberg, R. W. **2015**. A Closer Look into the Traditional Purification Process of CdSe Semiconductor Quantum Dots. *Langmuir*, *31*(49), 13433–13440.

(20) Jensen, F., Greer, A., & Clennan, E. L. **1998**. Reaction of Organic Sulfides with Singlet Oxygen . A Revised Mechanism, *7863*(12), 4439–4449.

9. ACRONYMS

2-NCA: 2-naphthoic acid

AFM: Atomic Force Microscope

CB: Conduction Band

CNT: Classical Nucleation Theory

e: electron

EET: Electronic Energy Transfer

Eg: Energy Gap

FWHM: Full-Width-at-Half-Maximum

h: hole

HDA: Hexadecylamine

HOMO: Highest Occupied Molecular Orbital

IC: Internal Conversion

ISC: Intersystem Crossing

IVR: Intramolecular Vibrational Redistribution

LUMO: Lowest Unoccupied Molecular Orbital

OA: Oleic Acid

ODE: 1-octadecene

QDs: Quantum Dots

QY: Quantum Yield

REET: Reversible Electronic Energy Transfer

STM: Scanning Tunneling Microscope

TAC: Time Amplitude Converter

TCSPC: Time Correlated Single Photon Counting

TOP: Trioctylphosphine

VB: Valence Band

VR: Vibrational Relaxation

APPENDICES

APPENDIX 1: PHOTOPHYSICAL CHARACTERIZATION OF 2-NAPHTHOIC ACID (2-NCA)

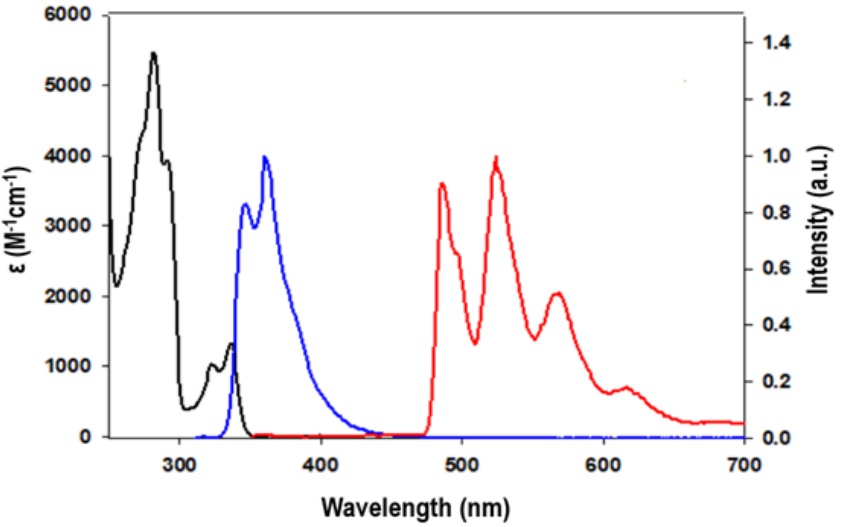

Absorption (black line) and fluorescence spectra (blue line, λexc = 300nm) recorded in DCM at room temperature; and phosphorescence spectrum (red line, λexc = 380nm) recorded in a rigid matrix (DCM: $CHCl_3$ = 1:1) at 77 K.

Absorption (ε) λmax	Fluorescence				Phosphorescence		
	λmax	Φ	τ	E S_1 (eV)	λmax	τ	ET_1(eV)
280 nm (6000 $M^{-1}cm^{-1}$)	347 nm	0.036	5,3 ns	3.63	487 nm	1,2 ns	2.58
323 nm (1000 $M^{-1}cm^{-1}$)	360 nm				525 nm		
336 nm (1600 $M^{-1}cm^{-1}$)					567 nm		
					618 nm		

Photophysical parameters of the 2-NCA.

APPENDIX 2: DATA FITTING OF THE LUMINESCENCE DECAYS

QDs sample	τ (%)	X^2
CdSe@2-NCA	111 ms (44.62 %) 543 ms (55.38 %)	1.13

QDs sample	τ (%)	X^2
CdSe@2-NCA	4.5 ns (24.84 %) 18 ns (42.66 %) 89.7 ns (32.30 %)	1.13

Data fitting of the luminescence decays in the milliseconds domain (top) and in the nanoseconds domain (below).